

Macroscopic Quantum Tunneling and Thermal Activation from Metastable States in a dc SQUID

F. Sharifi, J. L. Gavilano,^(a) and D. J. Van Harlingen

Department of Physics and Materials Research Laboratory, University of Illinois at Urbana-Champaign, Urbana, Illinois 61801

(Received 29 February 1988)

We have studied the transition rate from metastable wells in the two-dimensional potential of a dc SQUID as a function of applied flux and temperature. We observe a crossover from thermally activated escape to macroscopic quantum tunneling at a flux-dependent temperature. The thermal rates are significantly suppressed, suggesting that the potential barrier for activation is effectively enhanced by the interaction of the macroscopic degrees of freedom in the device.

PACS numbers: 74.50.+r, 03.65.-w, 05.40.+j, 85.25.Dq

Recently experiments have been carried out to test the validity of applying quantum mechanics to macroscopic physical systems. Motivated by theoretical work on macroscopic quantum phenomena and the role of dissipation in Josephson devices,¹⁻⁵ these experiments have involved measurements of the transition rate from the zero-voltage state of Josephson tunnel junctions⁶⁻⁸ or between different flux states in an rf SQUID.⁹ In a single junction, the condensate phase difference evolves in a one-dimensional "washboard" potential. In the zero-voltage state, the phase is trapped in a metastable potential well. When the device is current biased close to the thermodynamic critical current, escape can occur from the well either by thermal activation over the barrier or by macroscopic quantum tunneling (MQT) through the barrier. The crossover temperature T_c separating the regimes where each mechanism dominates depends on the parameters of the device; in particular, T_c is strongly reduced by damping.

In this Letter, we report a study of the thermal and quantum-tunneling transition rates in a dc SQUID. Experimentally, we find strong evidence for macroscopic quantum tunneling, characterized by a temperature-independent transition rate, below a crossover temperature T_c that is a strong function of flux bias. In the thermal-activation regime above T_c , the transition rate is significantly depressed, suggesting that the barrier height is effectively increased by the interaction of the degrees of freedom in the two-dimensional dc SQUID potential. In addition, we find evidence for substantial damping in our system which suppresses the MQT rate and induces quantum corrections to the thermal-activation rate.

Our interest in the dc SQUID is motivated by several factors. First, the two-dimensional potential allows two macroscopic degrees of freedom in the system, enabling us to investigate the dynamics and interaction of these variables. Second, the amplitude and shape of the potential barriers around a metastable minimum in the dc SQUID potential can be varied widely by application of external bias current and magnetic flux. The barrier form affects strongly the thermal-activation and quantum-tunneling rates and their dependence on dissipation.

Finally, we can use the applied magnetic flux as a control parameter to adjust the critical current of the dc SQUID and hence tune the transition rate. This is an important technique for switching between thermal and quantum-limited behavior and for optimizing device parameters in an experiment.

The system we have studied is a dc SQUID with loop inductance L and junctions of critical current $(1-\alpha)I_0$ and $(1+\alpha)I_0$; the parameter α allows for asymmetry in the critical currents. The potential-energy surface for a current bias $i=I/I_0$ and flux bias $f=\Phi/\Phi_0$ is given by¹⁰

$$U(\delta_1, \delta_2) = E_J [-(1-\alpha)\cos\delta_1 - (1+\alpha)\cos\delta_2 - \frac{1}{2}(\delta_1 + \delta_2)i + \frac{1}{2}\pi\beta j^2], \quad (1)$$

where $E_J = \hbar I_0 / 2e$ is the Josephson coupling energy and $j = (\delta_1 - \delta_2 - 2\pi f) / \pi\beta$ is the induced circulating current. Here δ_1 and δ_2 are the gauge-invariant junction phases and $\beta = 2LI_0 / \Phi_0$ is the inductance parameter. Energy contours for a symmetric SQUID with $i=0$ at $f=0$ and $f=\frac{1}{2}$ are shown in Fig. 1. The case shown is for $\beta \ll 1$, for which the saddle point over which thermal escape occurs lies on a line between adjacent potential wells. At zero flux bias, this path is the line $\delta_1 = \delta_2$; an increase of the flux bias shifts the wells and saddles in the δ_1 - δ_2 plane. For larger β , the potential is more complicated. The saddle point becomes a local maximum while two new saddles are formed on either side. The escape rate must include the rates through each saddle. We therefore chose to perform our measurements on a low-inductance SQUID.

We have fabricated dc SQUID's based on a Pb-alloy window junction technique. Junction areas of $0.8 \mu\text{m}^2$ separated by $2 \mu\text{m}$ are defined by the lifting off of windows in an SiO insulating layer on top of a Pb-In(12%)-Au(2%) base electrode. Following ion-mill cleaning of the base electrode and dc-glow-discharge oxidation, a Pb-Au(4%) counterelectrode is deposited to complete the junction and close the inductance loop. The (magnetic) loop area of $0.2 \mu\text{m}^2$ yields a SQUID self-inductance of 2.4 ± 0.1 pH, as determined from the SQUID modulation depth. We estimate the capacitance of each junc-

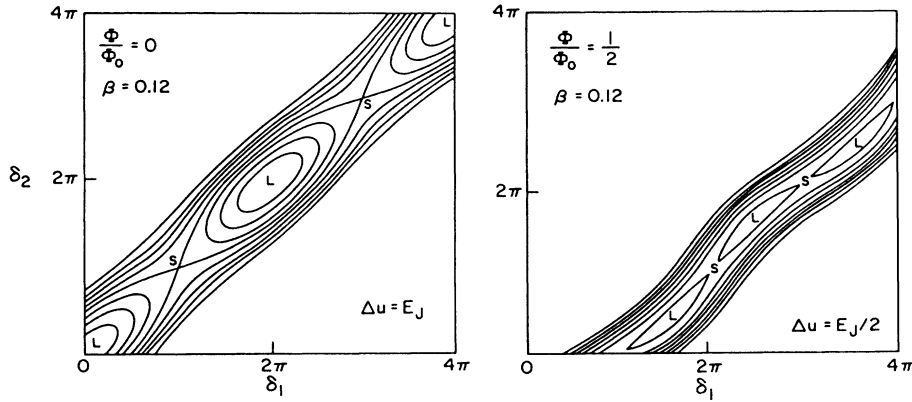


FIG. 1. Contour plots of the dc SQUID potential for zero current bias and flux biases of $f=0$ and $f=\frac{1}{2}$.

tion to be about 80 ± 20 fF; this value is obtained from the geometry based on oxide studies and from SQUID resonance measurements. We have made measurements on two SQUID's. Here we report results from a symmetric SQUID with $I_c = 2I_0 \approx 107 \mu\text{A}$ and $\beta = 0.12$; the other device had a critical current asymmetry $\alpha \approx 0.1$ and exhibited only minor differences from the symmetric sample. Measurements were obtained at temperatures from 50 mK to 1.7 K and at five flux biases of $f=0, \frac{1}{4}, \frac{1}{2}, \frac{3}{4},$ and 1; theoretically, the SQUID potentials at $f=1$ and $\frac{3}{4}$ are equivalent to those at $f=0$ and $\frac{1}{4}$, respectively, so that measurements at these flux values enable us to determine the modulation of the single-junction critical current by the applied field and test for flux noise from the magnetic field source.

In order to measure the escape rates for the SQUID, we monitor switching events from the zero-voltage to the finite-voltage state.¹¹ Distributions of switching currents $P(I)$ are obtained by our repeatedly ramping the bias current through the SQUID and recording the values at which a finite voltage appears with a multichannel analyzer. Typical distributions consist of 30000 to

50000 events sampled at 50 Hz. Since the current range in which these switching events occur is very narrow (typically $< 0.1\%$ of the device critical current), we offset and amplify the current scale to enhance our resolution. Junction self-heating is reduced by the switching off of the bias current immediately after the finite voltage appears, allowing the system to return to thermal equilibrium before the next transition is recorded. Shielding of the device from external noise is a major consideration in this experiment. Besides filtering all leads, the sample is enclosed in a superconducting (Pb foil) can and measurements are performed in an electromagnetically shielded room. A superconducting coil is placed around the substrate with the same orientation as the SQUID loop to apply external flux.

We characterize these distributions by calculating their first and second moments, $\langle I \rangle$ and σ , corresponding roughly to the peak and width of the distribution. Figure 2 shows the measured peaks and widths versus temperature for three flux biases. The data at $f=1$ and $f=\frac{3}{4}$ are essentially the same as the $f=0$ and $f=\frac{1}{4}$ results as expected, aside from a small suppression of the single-

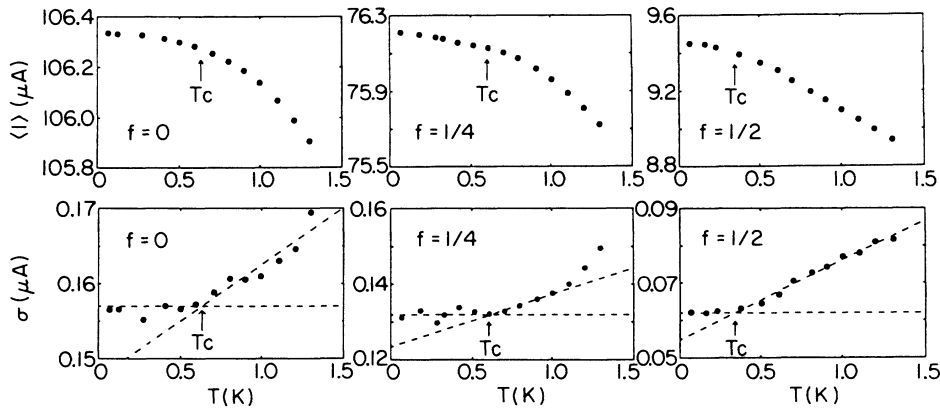


FIG. 2. Measurements of the transition-current distribution peaks $\langle I \rangle$ and widths σ vs temperature at flux biases $f=0, \frac{1}{4},$ and $\frac{1}{2}$. The dashed lines are guides to the eye used to define the crossover temperature T_c indicated by the arrows.

junction critical current by 12% at $f=1$. This indicates that external flux noise is not affecting the transition rate. We also note that the variation of the peaks with temperature at $f=\frac{1}{2}$ extends to below 100 mK, which puts an upper bound on the external noise from other sources. At each flux, the distribution width decreases roughly linearly as the temperature is lowered and flattens abruptly at a temperature we define as T_c (indicated by the arrow). The peak increases and eventually also flattens, but the transition is substantially rounded, increasing by typically 0.03% below T_c . This occurs because $\langle I \rangle$ is proportional to the transition rate, while σ is a measure of the variation of the rate with bias current and so is not as sensitive to changes in the prefactor that scale with I .⁹ The temperature independence of $\langle I \rangle$ and σ as T approaches zero is the signature of macroscopic quantum tunneling transitions from the zero-voltage state.

We have performed computer simulations to determine distribution peaks and widths as functions of temperature and flux bias for a two-dimensional thermal-activation model. The thermal transition rate is given by the usual form¹²

$$\Gamma_T = \Omega_T \exp(-\Delta U/k_B T), \quad (2)$$

where ΔU is the barrier height over the saddle and, in the two-dimensional case, the prefactor Ω_T is given for intermediate damping by¹³

$$\Omega_T = (\omega_{\parallel}\omega_{\perp}/2\pi\omega_{+})[(\eta^2/4+1)^{1/2} - \eta/2], \quad (3)$$

where $\eta=1/\omega-RC$ is the thermal damping factor. Here, ω_{\parallel} and ω_{\perp} correspond to the curvatures of the potential minimum along and transverse to the escape direction, and ω_{-} and ω_{+} correspond to the negative and positive curvatures (magnitudes) of the saddle.¹⁰ The thermal-activation rate is only weakly dependent on the damping. Therefore, the thermodynamic critical current, the only parameter in our system not independently determined, can in principle be obtained from the thermal data.

We and other groups⁶⁻⁸ have made measurements on single Josephson junctions which always give a good fit with the thermal-activation model and yield reasonable values of I_c . However, for the SQUID we are unable to fit our thermal results with any choice of I_c or any reasonable (or even unreasonable) adjustment of the other device parameters. The predicted temperature dependence (see curve labeled TA in Fig. 3) is considerably greater than we observe. In the thermal-activation model, the magnitude of the thermal transition rate is a strong function of the SQUID parameters, particularly the junction critical current, but the slope versus temperature is moderately insensitive to parameter changes. Our result indicates that the thermal-activation rate is significantly suppressed in the dc SQUID. In fact, we are only able to model our data accurately by assuming

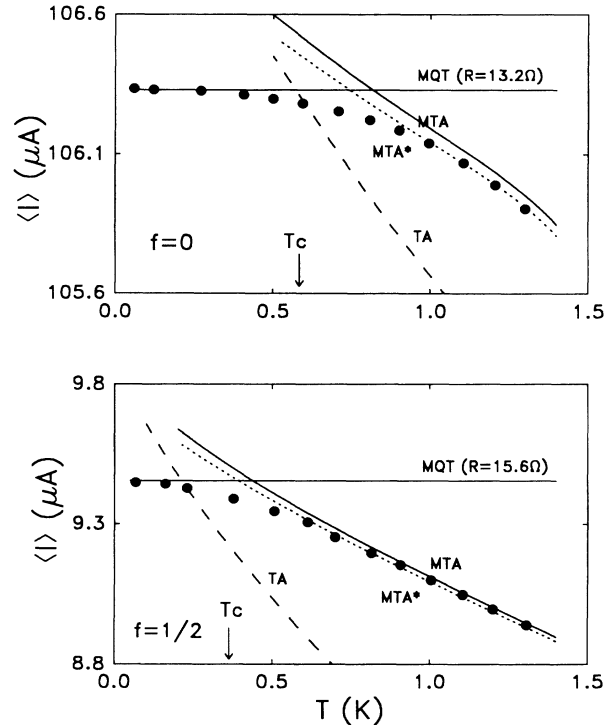


FIG. 3. Comparison of the peak data at $f=0$ and $f=\frac{1}{2}$ with a two-dimensional thermal-activation model (TA), and a modified thermal-activation model incorporating an enhanced barrier height without (MTA) and with (MTA*) quantum corrections to the thermal rate. Also plotted is the predicted MQT rate for the damping resistance indicated.

that the barrier height is effectively *increased* by a factor of about 2.5; using Eq. (3) with an enhanced barrier $\Delta U^*=2.5\Delta U$ we obtain the fit labeled MTA (modified thermal activation) in Fig. 3. We have no direct physical justification for such a barrier-height enhancement. However, Suhl¹⁴ has recently shown that under some conditions the thermal-activation rate in a multidimensional potential system can be significantly reduced from the usual Kramers prediction; there is some indirect evidence for this effect in chemical-reaction kinetics. This occurs because of coupling between the degrees of freedom in the system via the thermal bath that diverts thermal energy away from the mode capable of activating from the well. If we introduce this enhanced barrier height, we are able to fit our thermal results accurately well above T_c for all bias fluxes and extract a value for I_c . We also note that measurements of thermally induced transitions between different zero-voltage vortex states in Josephson interferometers^{15,16} have shown good agreement with the thermal-activation model, although the parameters of these devices are significantly different from those reported here.

We have not attempted a two-dimensional WKB or path-integral calculation to determine MQT rates for the

dc SQUID. However, for small β we expect the single-junction result^{2,5} to be a good approximation,¹⁷

$$\Gamma_Q = \Omega_Q \exp(-s\Delta U/\hbar\omega_{\parallel}), \quad (4)$$

where Ω_Q is the quantum-rate prefactor

$$\Omega_Q = \frac{\omega_{\parallel}}{2\pi} \left(\frac{\Delta U}{\hbar\omega_{\parallel}} \right)^{1/2} \chi. \quad (5)$$

The parameters s and χ are numerical factors that take into account dissipative and finite-temperature effects.⁵ We have taken ΔU to be the usual (unenhanced) barrier. Using this model, we find good agreement with the asymptotic peak value for an effective damping resistance of 15 Ω (slightly flux dependent); the undamped result ($\langle I \rangle = 105.2 \mu\text{A}$ at $f=0$, $8.8 \mu\text{A}$ at $f=\frac{1}{2}$) is well below that observed. This resistance value is comparable to the normal-state resistance of our SQUID. Previous experiments on unshunted junctions have also yielded damping resistances close to the normal-state value. This damping also couples thermal and quantum processes and may contribute to the rounding of the peak data in the crossover region. We have used a one-dimensional model⁷ to include the leading quantum corrections to the thermal rate above T_c in our simulations—quantum fluctuations enhance the rate by raising the metastable-state energy and by allowing tunneling through the remaining barrier when the particle is activated close to the top. These do yield an improved fit above T_c (dotted line labeled MTA* in Fig. 3) and may also account for the temperature dependence of the peak data below T_c . A full multidimensional quantum treatment is required to include these effects over the full crossover region. The quantum corrections are more evident compared to those in a single junction because of the suppressed thermal rate in the SQUID.

In conclusion, measurements of transition rates from zero voltage in a dc SQUID show strong evidence for macroscopic quantum tunneling. Damping substantially suppresses the MQT rate and broadens the crossover region to thermal activation. Most remarkably, we find that the thermal rate is suppressed. We are not able to explain this result but suggest that it may arise from the thermal-bath-mediated interaction of macroscopic degrees of freedom in the two-dimensional SQUID potential.

We are grateful to A. J. Leggett, Y.-C. Chen, G. C. Hilton, R. T. Wakai, K. N. Springer, and R. Felix for

valuable discussions and technical advice. This work was supported by the National Science Foundation through Grants No. NSF-DMR-84-11631 and No. NSF-DMR-87-22080. We also thank the University of Illinois Electron Beam Lithography Facility, and the Materials Research Laboratory for providing microfabrication and cryogenic facilities under National Science Foundation Grant No. NSF-DMR-86-12860.

(a)Present address: Institut de Physique, Université de Neuchâtel, Neuchâtel, Switzerland.

¹A. J. Leggett, *Prog. Theor. Phys.* **69**, 80 (1980), and in *Percolation, Localization, and Superconductivity*, edited by A. M. Goldman and S. Wolf, NATO Advanced Studies Institute, Series B, Vol. 109 (Plenum, New York, 1984).

²A. O. Caldeira and A. J. Leggett, *Ann. Phys. (N.Y.)* **149**, 374 (1983).

³L. D. Chang, and S. Chakravarty, *Phys. Rev. B* **29**, 2712 (1984).

⁴G. Schön, *SQUID '85, Superconducting Quantum Interference Devices and their Applications*, edited by H. Hahlbohm and H. Lubbig (de Gruyter, Berlin, 1985).

⁵H. Grabert, P. Olschowski, and U. Weiss, *Phys. Rev. B* **36**, 1931 (1987).

⁶L. D. Jackel, L. P. Gordon, E. L. Hu, R. E. Howard, L. A. Fetter, D. M. Tennant, R. W. Epworth, and J. Kurkijärvi, *Phys. Rev. Lett.* **47**, 697 (1981).

⁷R. F. Voss and R. A. Webb, *Phys. Rev. Lett.* **47**, 265 (1981); S. Washburn, R. A. Webb, R. F. Voss, and S. M. Faris, *Phys. Rev. Lett.* **54**, 2712 (1985).

⁸M. H. Devoret, J. M. Martinis, and John Clarke, *Phys. Rev. Lett.* **55**, 1908 (1985); M. H. Devoret, D. Esteve, J. M. Martinis, A. Cleland, and John Clarke, *Phys. Rev. B* **36**, 58 (1987).

⁹D. B. Schwartz, B. Sen, C. N. Archie, and J. E. Lukens, *Phys. Rev. Lett.* **55**, 1547 (1985).

¹⁰C. Tesche, *J. Low Temp. Phys.* **44**, 119 (1981).

¹¹T. A. Fulton and L. N. Dunkelberger, *Phys. Rev. B* **9**, 4760 (1974).

¹²H. A. Kramers, *Physica (Utrecht)* **7**, 284 (1940).

¹³E. Ben-Jacob, D. J. Bergman, Y. Imry, B. J. Matkowsky, and Z. Schuss, *J. Appl. Phys.* **54**, 6533 (1983).

¹⁴H. Suhl, *Phys. Rev. Lett.* **60**, 473 (1988).

¹⁵M. Naor, C. D. Tesche, and M. B. Ketchen, *Appl. Phys. Lett.* **41**, 202 (1982).

¹⁶M. Klein and A. Mukherjee, *Appl. Phys. Lett.* **40**, 744 (1982).

¹⁷Y.-C. Chen, *J. Low Temp. Phys.* **65**, 133 (1986).